Tohoku J. Exp. Med., 2022, **258**, 265-276

The SNHG1-Centered ceRNA Network Regulates Cell Cycle and Is a Potential Prognostic Biomarker for Hepatocellular Carcinoma

Lin Zhou,[1,2,*] Qing Zhang,[1,3,*] Haibin Deng,[1,4] Shuobo Ou,[1,4] Ting Liang[1,4] and Jianlin Zhou[1,4]

[1]State Key Laboratory of Developmental Biology of Freshwater Fish, College of Life Science, Hunan Normal University, Changsha, Hunan, China
[2]College of Clinical Laboratory, Changsha Medical University, Changsha, Hunan, China
[3]Reproductive and Genetic Hospital of CITIC-Xiangya, Changsha, Hunan, China
[4]Key Laboratory of Protein Chemistry and Developmental Biology of the Ministry of Education, College of Life Science, Hunan Normal University, Changsha, Hunan, China

Hepatocellular carcinoma (HCC) is one of the most common and lethal types of cancer. This study aimed to identify the expression regulatory network and a prognostic signature of HCC. RNA-seq data from The Cancer Genome Atlas were used to identify the differentially expressed genes (DEGs) between HCC and normal liver tissues. DEGs were subjected to the construction of protein-protein interaction (PPI) network and enrichment analysis of Gene Ontology terms and Kyoto Encyclopedia of Genes and Genomes pathways. The results showed that most of the DEGs were enriched in the cell cycle pathway, and the top 10 hub genes in the PPI network belong to the cell cycle pathway. A ceRNA network was constructed using starBase database, including one lncRNA (SNHG1), seven miRNAs (miR-195-5p, miR-199a-3p, miR-199a-5p, miR-199b-3p, miR-383-5p, miR-424-5p and miR-654-3p) and six of the top 10 hub genes (*BUB1*, *CCNA2*, *CCNB1*, *KIF11*, *NCAPG*, and *TOP2A*). *In vitro* experiments showed that knockdown of SNHG1 in the HCC cell lines (Huh7 and HepG2) decreased the expression of the six hub genes and cell viability, leading to cell cycle arrest at the G1 phase. These findings indicate that SNHG1 promotes cell proliferation by regulating cell cycle-related genes as a ceRNA. Additionally, Kaplan-Meier's survival and multivariate Cox regression analysis identified a prognostic signature of seven genes (including SNHG1 and the six SNHG1-regulated hub genes) for overall survival of HCC patients. In conclusion, this study identified a novel regulatory network in HCC and a potential independent prognostic factor for overall survival of HCC patients.

Keywords: cell cycle; ceRNA; hepatocellular carcinoma; lncRNA; SNHG1
Tohoku J. Exp. Med., 2022 December, **258** (4), 265-276.
doi: 10.1620/tjem.2022.J083

Introduction

Primary liver cancer is the sixth most commonly diagnosed cancer and the third leading cause of cancer-related deaths worldwide in 2020 (Sung et al. 2021). More than half of liver cancer cases occur in China (Yang et al. 2022). Hepatocellular carcinoma (HCC) is the most common form of primary liver cancer and accounts for approximately 90% of cases (Llovet et al. 2021). Because there are no specific clinical markers for early-stage HCC, 70-80% of patients are already at an advanced stage when they present with symptoms, missing the opportunity for radical resection (Li et al. 2018). Furthermore, the 5-year overall survival (OS) rate for HCC patients is only 12% in China (Zheng et al. 2018). Therefore, it is necessary to discover new biomarkers and molecular targets for the diagnosis and prognosis of HCC.

Variations in gene expression patterns have been

Received August 31, 2022; revised and accepted October 2, 2022; J-STAGE Advance online publication October 14, 2022
*These two authors contributed equally to this work.
Correspondence: Jianlin Zhou, State Key Laboratory of Developmental Biology of Freshwater Fish, College of Life Science, Hunan Normal University, Changsha, Hunan 410081, China.
e-mail: jlzhou@hunnu.edu.cn

shown to be associated with the pathogenesis of HCC and to have prognostic significance (Yang et al. 2021). Serum alpha-fetoprotein (AFP) is the most commonly applied molecular marker for screening, diagnosis, and treatment of HCC (Pinero et al. 2020). Recently, researchers have shown that the expression signature of protein-coding or noncoding genes in HCC tissues may be used as prognostic markers (Wang and Zhang 2021; Yang et al. 2021; Kong et al. 2022).

Although noncoding RNAs (ncRNAs) lack protein-coding capabilities, they are found in all organisms (Yamamura et al. 2018). As a subspecies of ncRNAs, long noncoding RNAs (lncRNAs) with a length greater than 200 nt were previously considered to be transcriptional noise (Quinn and Chang 2016). However, there is growing evidence that lncRNAs play pivotal roles in tumor-related processes, including proliferation, invasion, and metastasis (Sana et al. 2012; Takahashi et al. 2014; Ba et al. 2018). LncRNAs are involved in transcriptional regulation, chromatin modification, and alternative splicing in the nucleus. In the cytoplasm, lncRNAs affect the stability and/or translation of mRNA as microRNA (miRNA) sponges (also called competitive endogenous RNAs, ceRNAs) (Cao et al. 2021). The ceRNA hypothesis was proposed by Salmena et al. (2011). If a lncRNA shares the same miRNA response elements (MREs) with an mRNA, it may bind competitively to the miRNA, thereby inhibiting the action of miRNA on that mRNA (Salmena et al. 2011). Several studies have shown that lncRNAs play a crucial role in the occurrence and progression of HCC as ceRNAs (Di Palo et al. 2020; Xu et al. 2020).

In the present study, we first identified differentially expressed lncRNAs (DElncRNAs), miRNAs (DEmiRNAs), and RNAs [DEmRNAs, responding to protein-coding genes (DEGs)] in HCC through data-mining of The Cancer Genome Atlas (TCGA) database. A protein-protein interaction (PPI) network of DEGs was then generated, and the ten hub genes in the network were identified. Correlation analysis revealed that the expression of the lncRNA SNHG1 was significantly and positively correlated with the expression of all ten hub genes. StarBase database was used to predict lncRNA-miRNA and miRNA-mRNA pairs. Finally, a SNHG1-miRNAs (miR-195-5p, miR-199a-3p, miR-199a-5p, miR-199b-3p, miR-383-5p, miR-424-5p and miR-654-3p)-mRNAs (*BUB1, CCNA2, CCNB1, KIF11, NCAPG* and *TOP2A*) network was constructed. A seven-gene signature that predicts the OS rate of HCC patients was also established.

Materials and Methods

RNA-Seq data collection

The GDC TCGA-LIHC cohort's gene expression RNAseq data (374 cases of HCC tissues vs. 50 cases of adjacent normal liver tissues), TCGA-LIHC cohort's miRNA expression RNA-seq data (371 cases of HCC tissues vs. 49 cases of adjacent normal liver tissues), and correlating phenotype data were downloaded from the UCSC Xena Browser (https://xenabrowser.net).

Identification of differentially expressed RNAs

The DElncRNAs, DEmiRNAs, and DEmRNAs between HCC tissues and adjacent normal liver tissues were identified using the 'limma' package of the R software. The threshold for DEmRNA was |log2 (fold change)| $\geq$ 2 and adj. p-value < 0.05, the threshold for DElncRNA and DEmiRNA was |log2 (fold change)| $\geq$ 1.5 and adj. p-value < 0.05. Heatmap and volcano plot were visualized using the R package 'pheatmap' and 'ggplot2', respectively.

Functional enrichment analysis

Enrichment analysis of gene ontology (GO) terms and KEGG (Kyoto Encyclopedia of Genes and Genomes) pathway were performed using DAVID database (https://david.ncifcrf.gov/). $p<0.05$ was defined as statistically significant. Gene set enrichment analysis (GSEA) was performed using the 'clusterProfiler' package and visualized using the 'ggplot2' and 'enrichplot' package in R software (version 4.1.0). The terms satisfying a threshold of normalized enrichment score (NES) >1 or <1 and p-value < 0.05 were considered to be significantly enriched.

Identification of hub genes

The PPI network was constructed for DEGs using STRING (https://string-db.org/). The PPI pairs with an interaction score $\geq$ 0.7 were visualized in the network. The cytoHubba plugin based on Cytoscape (Version 3.9.1) was used to identify highly connected hub genes in the PPI network. Finally, the top 10 genes with the highest degree of connectivity in the PPI network were selected as hub genes.

Construction of the ceRNA network

Based on the ceRNA hypothesis, a ceRNA network was constructed in the following steps: co-expression analysis between the ten hub genes and DElncRNAs was performed using psych package in R software to identify lncRNA-mRNA co-expression pairs. Then, the StarBase database (https://starbase.sysu.edu.cn/index.php) was employed to predict potential lncRNA-miRNA and miRNA-mRNA pairs. The ceRNA network was visualized using the Cytoscape software.

Construction of a prognostic signature and nomogram

Univariate and multivariate Cox regression analysis was performed to explore the association between gene expression and overall survival (OS) using the survival package in R software. Then, the risk score of every patient was calculated based on the coefficient of multivariate Cox regression analysis, and the samples were divided into high- and low-risk groups using the median risk score as a cutoff. The Kaplan-Meier analysis was performed to compare OS curves between the two groups. The time-dependent receiver operating characteristic (ROC) curve was used to

evaluate the predictive value of the prognostic signature. A nomogram was constructed to evaluate the probability of 1-year, 3-year, and 5-year overall survival in HCC patients using the 'rms' package in R software.

Cell lines and culture

The HCC cell lines HepG2 and Huh7 were obtained from ATCC (Manassas, VA, USA) and cultured according to the instruction of ATCC. All the cell lines were mycoplasma-free and authenticated using short tandem repeats analysis by Yubo Biological Technology Co., Ltd. (Shanghai, China).

Lentivirus infection

The lentiviruses expressing SNHG1 shRNA and scrambled shRNA were purchased from GeneChem (Shanghai, China). The target sequence of SNHG1 shRNA (5′-GTTTGCTGTGTATCACATTTCT-3′) has been validated to be effective by Sun et al. (2017). Lentivirus particles were transduced into cells according to the manufacturer's instruction. At 72 h after transduction, cells were cultured in the fresh medium containing hygromycin B to generate stable cell lines.

Western blotting

Total cellular protein was extracted using radioimmunoprecipitation (RIPA) buffer (Thermo Fisher Scientific, Waltham, MA, USA) according to the manufacturer's instruction. Proteins were separated by 12% sodium dodecyl sulfate (SDS)-polyacrylamide gel electrophoresis (PAGE) and transferred to a polyvinylidene difluoride (PVDF) membrane. After blocking, the membrane was cut into pieces to incubate with antibodies separately. All the primary antibodies and horseradish peroxidase (HRP)-conjugated secondary antibodies were purchased from ABclonal Technology (Wuhan, China). The protein bands were visualized using ChemiLucent ECL Detection System (Millipore, Billerica, MA, USA).

RNA isolation and reverse-transcription quantitative PCR (RT-qPCR)

Total RNA was isolated from cell lines using TRIzol reagent (Invitrogen, Carlsbad, CA, USA) and then reverse-transcribed into cDNA using All-in-One™ First-Strand cDNA Synthesis Kit (GeneCopoeia, Guangzhou, China). SYBR green-based real-time qPCR was performed in ABI 7900 thermocycler (Thermo Fisher Scientific). The primers were as follows: 18s rRNA, 5′-CGGCGACGACCCATTCGAAC-3′ (forward) and 5′-GAATCGAACCCTGATTCCCCGTC-3′ (reverse); SNHG1, 5′- GCCAGCACCTTCTCTCTAAAGC-3′ (forward) and 5′- GTCCTCCAAGACAGATTCCATTTT-3′ (reverse).

Flow cytometry

The cell cycle was analyzed by a propidium iodide (PI) staining kit (Muti Sciences, Hangzhou, China) according to the manufacturer's instructions. After staining, the different stages of the cell cycle were analyzed using a flow cytometer (CytoFlex, Beckman Coulter, Fullerton, CA, USA).

MTT [3- (4,5-dimethylthiazol-2-yl)-2,5 diphenyl tetrazolium bromide] assay

Cells were plated on 96-well plates for the indicated time. Then, the cells were cultured in the serum-free media with MTT reagent (0.5 mg/mL) for 4 h. Media were removed, and 100 μL dimethyl sulfoxide (DMSO) was added to solubilize formazan crystals. Absorbance was measured at 490 nm in a Biotek Synergy 2 plate reader (Biotek, Winooski, VT, USA).

Statistical analysis

R software (version 4.1.0) was used for statistical analysis. Pearson's correlation coefficient was calculated to assess correlations. Student's t test was used to compare the difference of expression between two groups. Log-rank test was performed to evaluate the significance of the difference in survival curves. The value was shown as mean ± SD. A p-value < 0.05 was considered to be statistically significant.

Results

Cell cycle-related genes are significantly upregulated in HCC tissues

According to the differential expression analysis, 634 DElncRNAs (488 upregulated and 146 downregulated), 52 DEmiRNAs (12 upregulated and 40 downregulated), and 1,000 DEGs (551 upregulated and 449 downregulated) were identified between the tumor and adjacent normal tissues. The distributions and expression patterns of the DERNAs were displayed using volcano plots and heatmaps in Fig. 1A-C.

The 1,000 DEGs were subjected to GO and KEGG enrichment analysis. The top 3 enriched GO terms in the biological process were sister chromatid cohesion, cell division, and mitotic nuclear division (Fig. 2A, Supplementary Table S1). All these biological processes belong to the cell cycle pathway. Consistent with GO analysis, enrichment analysis of KEGG pathway by DAVID revealed that DEGs were most enriched in the cell cycle pathway (Fig. 2B, Supplementary Table S2). GSEA analysis showed that the cell cycle pathway was the most upregulated pathway in HCC (Fig. 2C, D, Supplementary Table S3). The results suggest that activation of the cell cycle pathway may be the main driving force of HCC.

The hub genes of DEGs are overexpressed in HCC and play roles in the cell cycle pathway

A PPI network of 1,000 DEGs was constructed using the STRING database. In the PPI network, the top 10 genes with the highest degree of connectivity (according to a degree from high to low: *CDK1, CCNA2, BUB1, CCNB1, TOP2A, NCAPG, BUB1B, CDC20, KIF11, CCNB2*) were

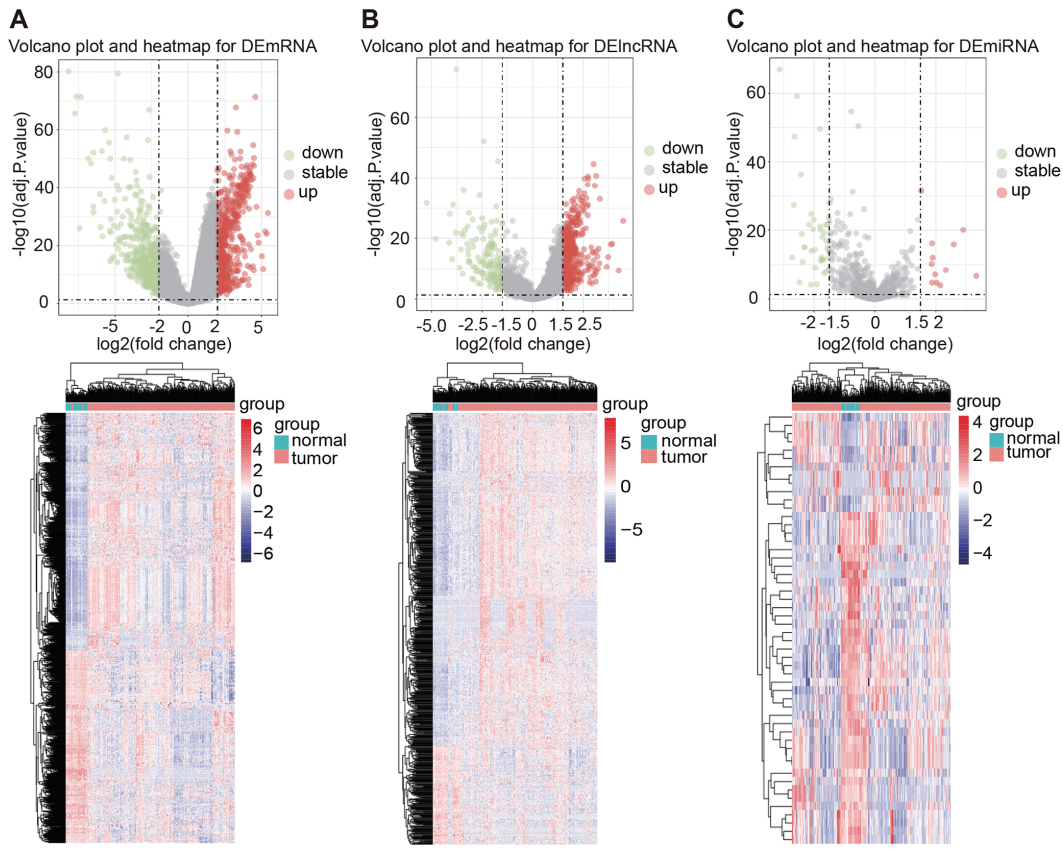

Fig. 1. Volcano plots and heatmaps for the differentially expressed RNAs (DERNAs). (A) Differentially expressed mRNAs (DEmRNAs). (B) Differentially expressed long noncoding RNAs (DElncRNAs). (C) Differentially expressed microRNAs (DEmiRNAs). The volcano plots and heatmaps are shown in upper and lower panels, respectively.

defined as hub genes (Fig. 3A, B). Interestingly, all these hub genes were significantly upregulated in HCC according to TCGA data (Fig. 4). According to the above enrichment analysis (Supplementary Tables S1-3), all these hub genes belong to the cell cycle-related genes. These results indicated that the cell cycle pathway plays a crucial role in the pathogenesis of HCC.

SNHG1 upregulates six hub genes as a ceRNA

To explore the upstream regulatory mechanism of hub genes, we established a lncRNA-miRNA-mRNA network in HCC. Firstly, we investigated the co-expression correlation between the 10 hub genes and DElncRNAs and found that the lncRNA SNHG1 was overexpressed in HCC and highly positively correlated with each hub gene (Fig. 5A, B). According to the ceRNA hypothesis (Salmena et al. 2011), miRNA and mRNA/lncRNA are negatively correlated in the ceRNA network. Thus, the miRNAs targeting both SNHG1 and hub genes were searched from the 40 downregulated DEmiRNAs using starBase database (Fig. 5C). A total of seven miRNAs (miR-195-5p, miR-199a-3p, miR-199a-5p, miR-199b-3p, miR-383-5p, miR-424-5p and miR-654-3p) were found to bind potentially to both SNHG1 and one or two of six hub genes (Fig. 5D). Based on the above results, we identified a ceRNA network: SNHG1-miRNAs (miR-195-5p, miR-199a-3p, miR-199a-5p, miR-199b-3p, miR-383-5p, miR-424-5p and miR-654-3p)-mRNAs (*BUB1, CCNA2, CCNB1, KIF11, NCAPG* and *TOP2A*) (Fig. 5D).

Experimentally validating the regulatory role of SNHG1 on hub genes and cell cycle

To validate the roles of SNHG1, we silenced the expression of SNHG1 in the HCC cell lines Huh7 and HepG2 by a lentivirus-mediated shRNA system (Fig. 6A). We then investigated the influence of SNHG1 expression on hub genes and cell cycle. Western blotting showed that knockdown of SNHG1 in both Huh7 and HepG2 cells decreased the protein levels of six hub genes (Fig. 6B). It indicated that SNHG1 upregulated the expression of these genes. Flow cytometric assay showed that after knockdown of SNHG1, the proportion of cells in the G1 phase significantly increased, while the proportion of cells in the S phase decreased (Fig. 6C, D). This result indicates that the cell cycle was blocked in the G1 phase. MTT assay further demonstrated that knockdown of SNHG1 significantly decreased cell proliferation (Fig. 6E). These results confirmed that SNHG1 upregulates the six hub genes and then promotes the cell cycle.

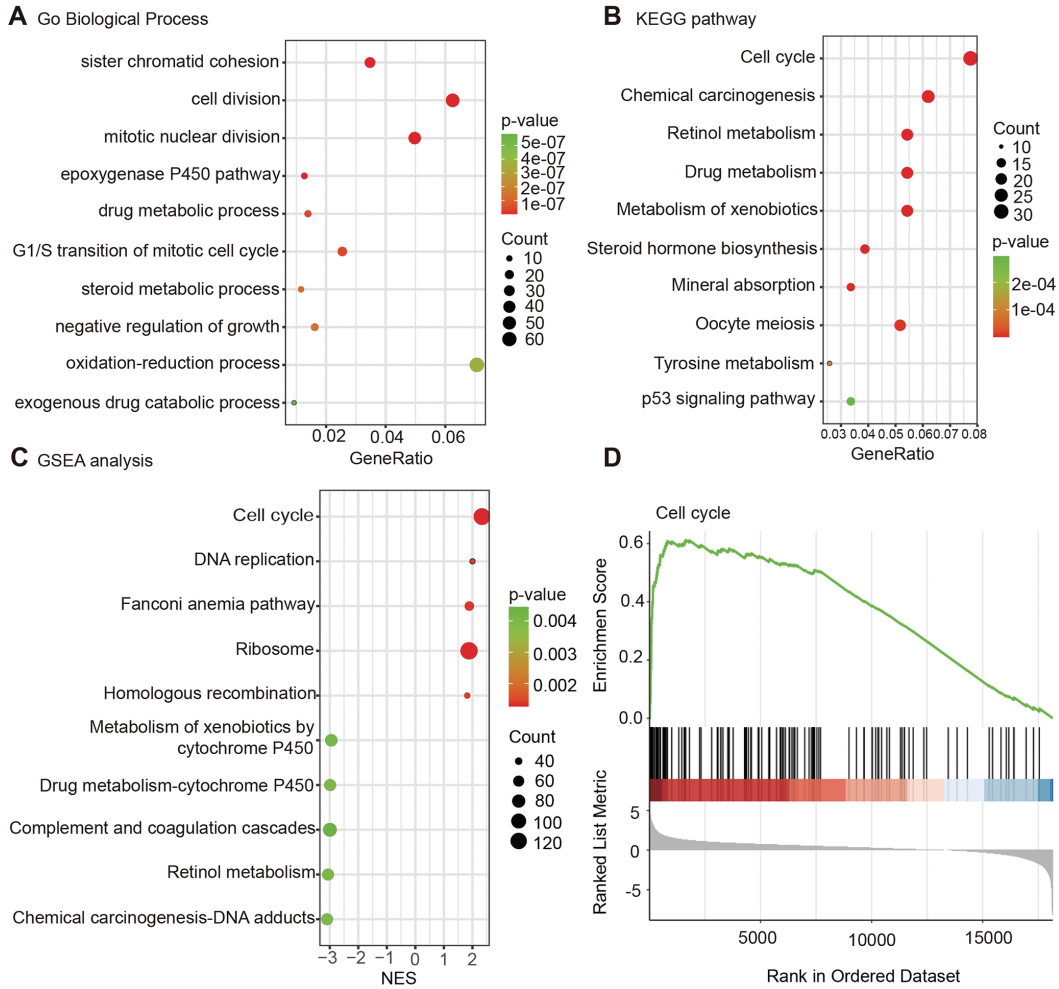

Fig. 2. Enrichment analysis of the differentially expressed genes (DEGs).
(A) Top 10 significant gene ontology (GO) terms in the biological process identified by DAVID. (B) Top 10 significant KEGG (Kyoto Encyclopedia of Genes and Genomes) pathways identified by DAVID. (C) Top 5 downregulated and top 5 upregulated KEGG pathways identified by the gene set enrichment analysis (GSEA). (D) An enrichment plot generated by GSEA analysis of ranked gene expression data (red, upregulated; blue, downregulated).

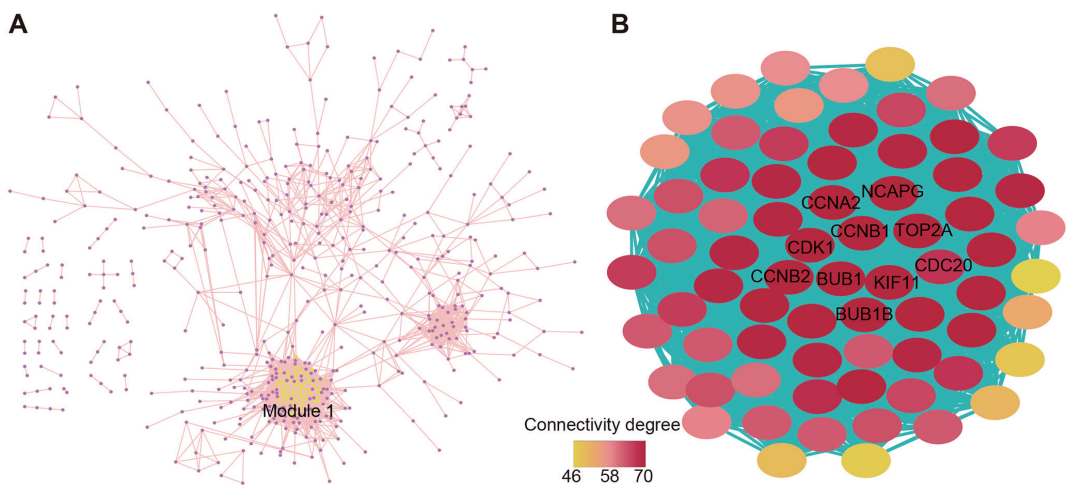

Fig. 3. The protein-protein interaction (PPI) network showed the top 10 hub genes of the significant differentially expressed genes (DEGs).
(A) The whole PPI network of DEGs. The proteins in Module 1 are highlighted in yellow. (B) The PPI network of Module 1. The hub genes are labeled, other genes are shown as dots and all interactions are shown as lines.

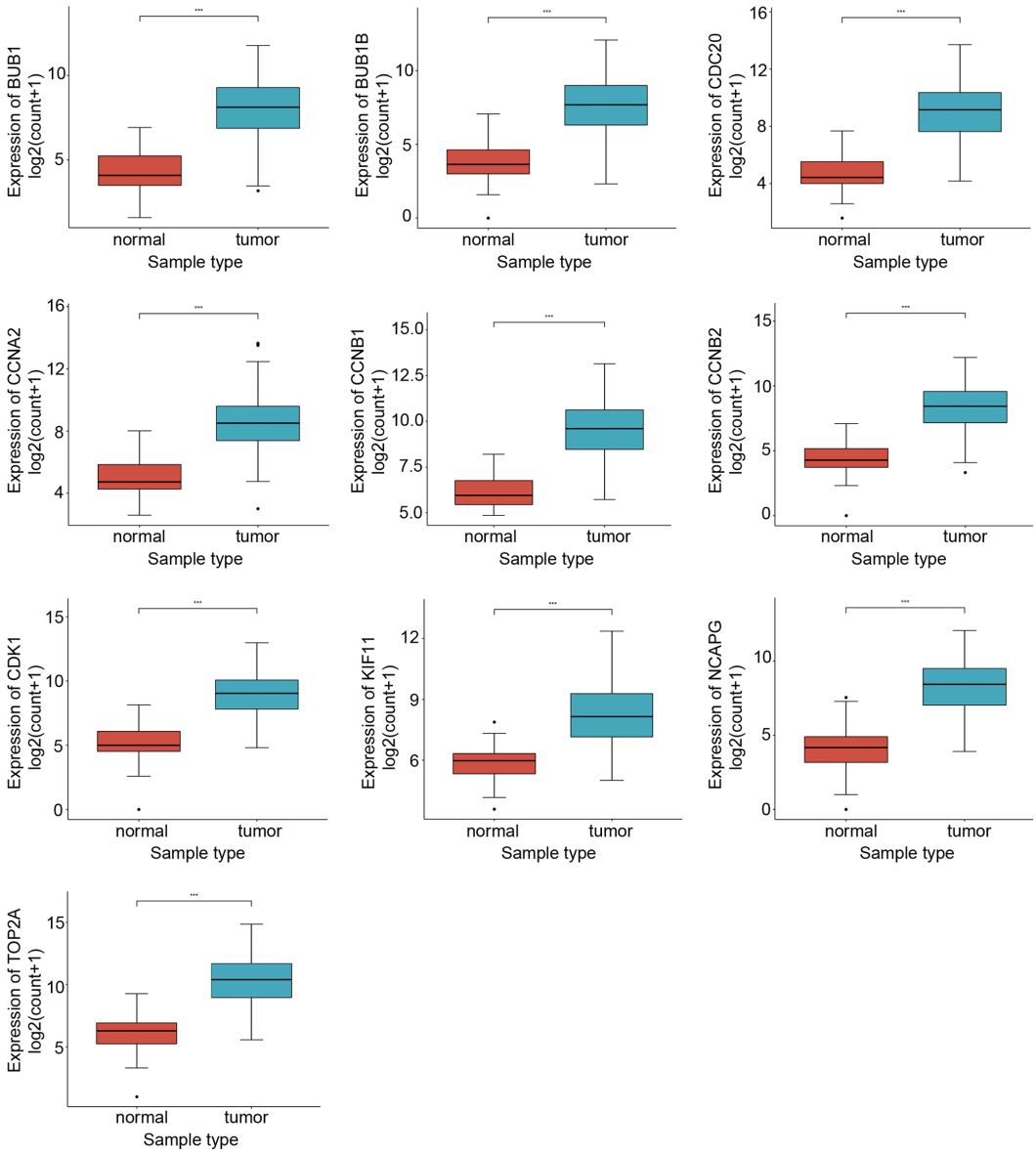

Fig. 4. Differential expressions of hub genes between hepatocellular carcinoma (HCC) tissues and adjacent normal liver tissues.
Analysis of differential expression was performed using the GDC TCGA-LIHC cohort's gene expression RNAseq data (374 cases of HCC tissues vs. 50 cases of adjacent normal liver tissues). All the values were presented as means ± SD.

Construction and validation of a prognostic signature constructed by SNHG1 and six SNHG1-regulated genes

To explore the prognostic significance of the ceRNA network, we investigated the prognostic significance of the seven genes (*SNGH1* and the six SNGH1-regulated genes: *BUB1, CCNA2, CCNB1, KIF11, NCAPG* and *TOP2A*) in the ceRNA network using the clinical parameters and expression data from TCGA database. The results showed that overexpression of any gene was significantly positively associated with increased stage, grade, and local tumor stage (Supplementary Table S4). Kaplan-Meier survival and Univariate Cox regression analysis showed that each of the seven genes was significantly associated with OS of HCC patients (Table 1, Fig. 7). Then, these seven genes were used to construct a prognostic model to predict OS of HCC patients. The risk score of every patient was calculated based on the coefficient of multivariate Cox regression analysis (Table 1): risk score = 0.046* Exp (SNHG1)+ 0.132* Exp (NCAPG)+0.192* Exp (CCNB1)+0.046* Exp (KIF11)+0.022* Exp (CCNA2)-0.281* Exp (TOP2A)+0.212* Exp (BUB1), where "Exp" denoted the expression level of mRNA. To assess whether the risk score has prognostic significance, we explored the relationship between risk score and clinicopathological characteristics. HCC patients were divided into high- and low-risk groups according to the median risk score. Correlation analysis showed that risk score was significantly correlated with stage, grade, and local tumor stage but not with age,

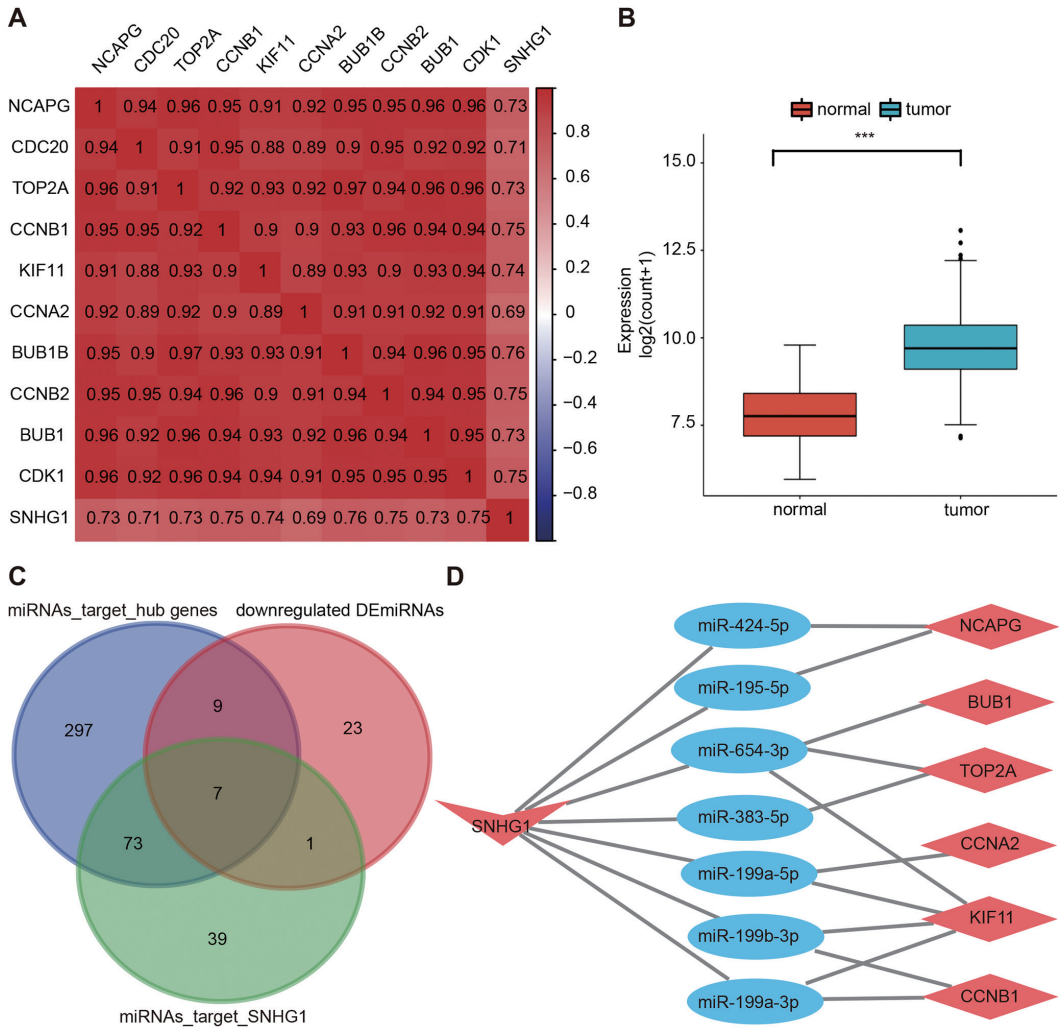

Fig. 5. Construction of a ceRNA network.
(A) Heatmap of the correlation between SNHG1 expression and expression of each hub gene. The numbers in the grid denote the Spearman correlation coefficients. (B) Differential expression of SNHG1 between HCC tissues and adjacent normal liver tissues based on the GDC TCGA-LIHC cohort's gene expression data (374 cases of HCC tissues vs. 50 cases of adjacent normal liver tissues). The values were presented as means ± SD. (C) Venn diagram showing the numbers of the predicted miRNAs targeting hub genes/SNHG1 and the downregulated DEmiRNAs. (D) A ceRNA network of lncRNA-miRNA-mRNA.

sex, node status, or metastasis status (Table 2). The KM survival curve demonstrated that patients in the high-risk group had significantly poorer outcomes compared with those in the low-risk group (Fig. 8A). The time-dependent ROC curve analysis showed that the area under curve (AUC) of 1-year, 3-year, and 5-year survival predicted by the prognostic signature (risk score) was 0.709, 0.675, and 0.654, respectively, indicating good performance of the seven-gene signature for OS prediction (Fig. 8B). These results indicated that the risk score based on the expression of the seven genes is an independent prognostic factor for OS of HCC patients.

Construction of a prognostic nomogram

Furthermore, multivariate Cox regression analysis was performed based on factors including age, sex, stage, grade, TNM stage, and risk score. The results showed that risk scores are independent prognostic factors for the OS of HCC (Fig. 8C). A nomogram based on risk score was then constructed to evaluate the probability of 1-year, 3-year, and 5-year overall survival in HCC patients (Fig. 8D).

Discussion

Variation in gene expression patterns is a common feature in cancer tissues, and the expression pattern in cancer tissues has prognostic significance (Yang et al. 2021). The present study systematically analyzed DEGs between HCC and adjacent normal tissues by mining the TCGA data and identified a total of 1,000 DEGs. Enrichment analysis of GO, KEGG, and GSEA showed that DEGs were most significantly enriched in the cell cycle pathway. Among the PPI network of DEGs, ten genes (*BUB1, BUB1B, CCNA2,*

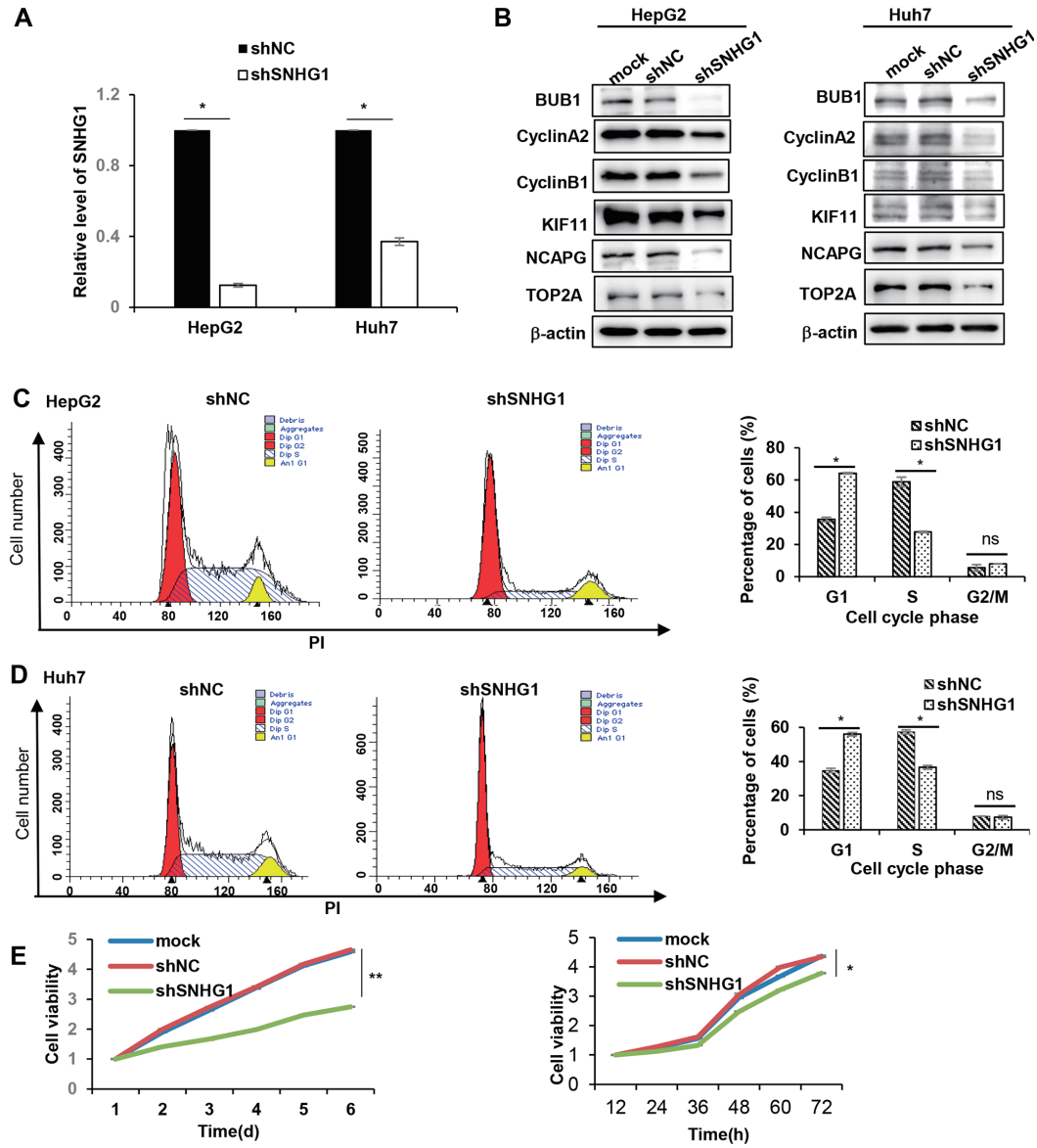

Fig. 6. Experimental validation of the influence of SNHG1 on hub genes and cell proliferation. (A) qRT-PCR analysis of SNHG1 levels in the untreated cells (mock) and the cells with stably expressing SNHG1 shRNA (shSNHG1) or scrambled shRNA (shNC). (B) Western blotting analysis of the influence of SNHG1 knockdown on the protein levels of hub genes. (C,D) Flow cytometric analysis of the influence of SNHG1 knockdown on cell cycle. Representative images and corresponding statistical plots were shown in the left and right panels, respectively. (E) MTT assay analysis of the influence of SNHG1 knockdown on cell proliferation. All the values were presented as means ± SD for three independent experiments.

CCNB1, CCNB2, CDC20, CDK1, NCAPG, KIF11, TOP2A) were identified as hub genes. This result is partially consistent with the finding of Tan et al. (2022). Four of these hub genes (*BUB1B, CCNB1, CDK1* and *TOP2A*) were also identified as the hub genes in the network of upregulated genes in Hepatitis B virus-related HCC (Tan et al. 2022). Interestingly, all these hub genes were upregulated in HCC tissues and have been reported to play roles in the cell cycle process. Both BUB1 and BUB1B (also termed BUBR1) are kinases critical for chromosome alignment during the spindle assembly checkpoint (SAC) (Bolanos-Garcia and Blundell 2011; Elowe and Bolanos-Garcia 2022). Both CCNA2 and CCNB1 bind and activate CDK1. CDK1 interacts with CCNA2 to regulate S phase entry partially through TOP2A phosphorylation and interacts with CCNB1 to regulate M phase progression (Jin et al. 2021). CDK1/CCNB1 complex creates a spindle checkpoint-permissive state and drives mitotic spindle assembly (Hayward et al. 2019; Serpico et al. 2022). CDC20 is an activator of the anaphase-promoting complex/cyclosome (APC/C), which is required for sister-chromatid separation and the transition into anaphase (Kapanidou et al. 2017). KIF11 is a spindle motor protein required for the maintenance of the spindle chirality in metaphase (Novak et al. 2018). NCAPG, a sub-

Table 1. Univariate and multivariate Cox regression analysis of the seven genes in ceRNA on overall survival of hepatocellular carcinoma (HCC).

Genes	Univariate analysis			Multivariate analysis		
	coefficients	HR (95% CI)	p-value	coefficients	HR (95% CI)	p-value
SNHG1	0.299	1.35 (1.13-1.61)	1.11E-03	0.046	1.05 (0.83-1.32)	0.70
NCAPG	0.263	1.30 (1.16-1.46)	6.08E-06	0.132	1.14 (0.77-1.70)	0.52
CCNB1	0.314	1.37 (1.21-1.55)	1.15E-06	0.192	1.21 (0.87-1.69)	0.26
KIF11	0.265	1.30 (1.15-1.47)	2.17E-05	0.046	1.05 (0.71-1.54)	0.82
CCNA2	0.208	1.23 (1.12-1.36)	3.67E-05	0.022	1.02 (0.81-1.29)	0.85
TOP2A	0.193	1.21 (1.10-1.34)	9.36E-05	−0.281	0.76 (0.52-1.09)	0.13
BUB1	0.259	1.30 (1.16-1.45)	5.61E-06	0.212	1.24 (0.80-1.91)	0.34

HR, hazard ratio; CI, confidence interval.

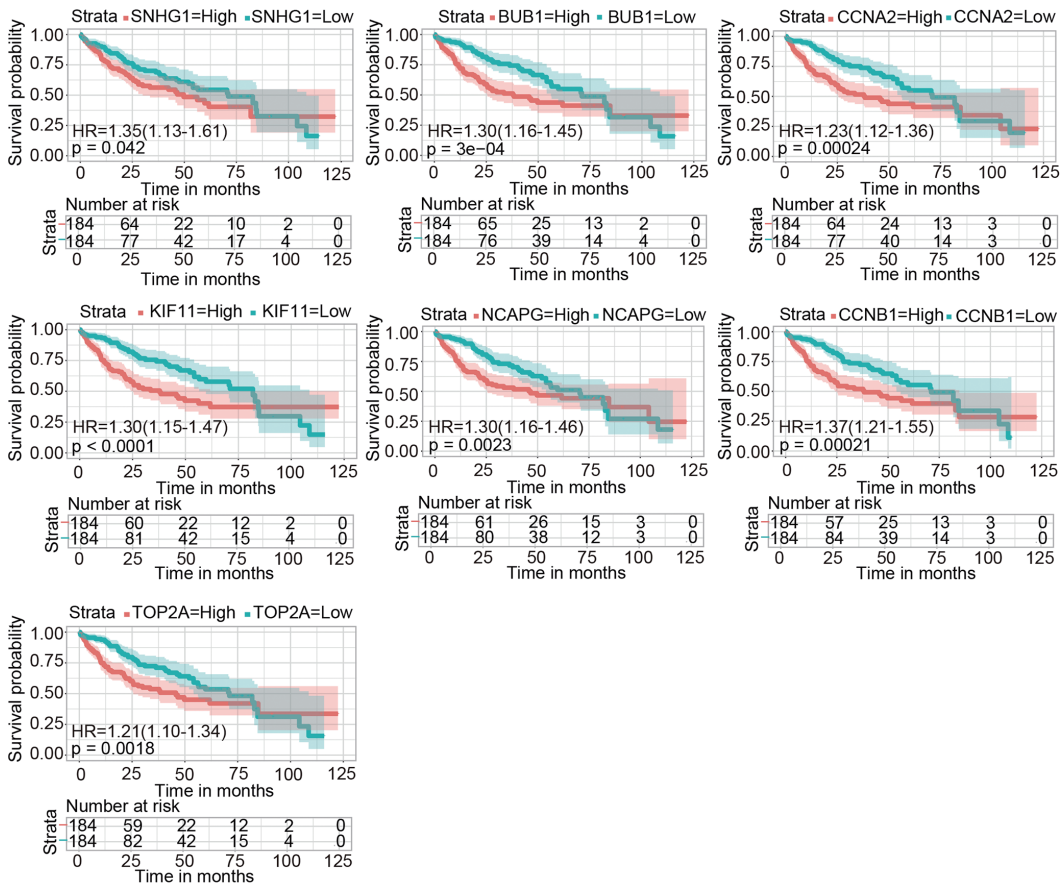

Fig. 7. Correlation of mRNA levels and overall survival in HCC patients.
Kaplan-Meier survival curve analysis was performed using clinical data from the TCGA database (374 cases of HCC tissues vs. 50 cases of adjacent normal liver tissues).

unit of the condensin complex, is responsible for the condensation and stabilization of chromosomes during mitosis (Hara et al. 2019). TOP2A is a type II topoisomerase that is crucial for maintenance of mitotic chromosomes (Nielsen et al. 2020). These results suggested that ectopic expressions of the cell cycle-related genes play vital roles during the occurrence and development of HCC.

The expressions of protein-coding genes are often regulated by ncRNAs, such as miRNAs and lncRNAs. MiRNAs can suppress the translation or/and stability of mRNA, and ncRNAs can relive the inhibition of miRNA on mRNA as ceRNAs (Cao et al. 2021). To elucidate the mechanism underlying the aberrant expression of the hub genes, we generated a ceRNA network by analyzing correlations among DEGs, DEmiRNAs, and DElncRNA in the TCGA database and predicting lncRNA-miRNA and miRNA-mRNA pairs using the StarBase database. We found that SNHG1 can upregulate six hub genes (*BUB1,*

Table 2. Correlation between risk score and clinical parameters in hepatocellular carcinoma (HCC) patients.

Parameters	Number	High	Low	p-value
Age				0.1219
< 60	121	70	51	
> = 60	112	46	66	
Sex				0.2435
Male	161	76	85	
Female	72	40	32	
Tumor stage				0.0083
I+II	164	75	89	
III+IV	69	41	28	
Tumor grade				0.0004
G1+G2	130	53	77	
G3+G4	103	63	40	
TNM stage				
Local tumor (T)				0.0068
T1+T2	167	76	91	
T3+T4	66	40	26	
Node (N)				0.9445
N0	229	114	115	
N1	4	2	2	
Metastasis (M)				0.4753
M0	230	116	114	
M1	3	0	3	

CCNA2, CCNB1, KIF11, NCAPG and *TOP2A*) by sponging miRNAs (miR-195-5p, miR-199a-3p, miR-199a-5p, miR-199b-3p, miR-383-5p, miR-424-5p and miR-654-3p).

SNHG1 has been well recognized to be an oncogenic lncRNA that contributes to cell proliferation, invasion, and metastasis of cancer cells (reviewed in Thin et al. 2019). Several *in vitro* experiments also demonstrated that SNHG1 could play roles in HCC as a ceRNA (Li et al. 2020; Qu and Yang 2020; Meng et al. 2021; Mu et al. 2021). However, the role and mechanism of SNHG1 have not been systematically investigated in HCC. The present study demonstrated that upregulation of the cell cycle-related genes is the most significant change in gene expression in HCC. Moreover, all the ten hub genes belonged to cell cycle-related genes. Among these hub genes, six are upregulated by SNHG1. *In vitro* experiments further confirmed that knockdown of SNHG1 in both Huh7 and HepG2 cells decreased the protein levels of six hub genes and cell viability, leading to cell cycle arrest at G1 phase. These results indicated that SNHG1 plays a critical role in the regulation of cell cycle in HCC.

At last, we evaluated the prognostic significance of SNHG1 and the six genes regulated by SNHG1, and found that all these seven genes were significantly associated with OS. Consistent with our findings, many reports have shown that expressions of these genes were closely related to HCC (Wong et al. 2009; Xu et al. 2017; Gong et al. 2019; Li et al. 2019; Jin et al. 2020; Qiu et al. 2020; Hu et al. 2021; Liu et al. 2021; Zhao et al. 2021). Meanwhile, a seven-gene signature constructed by SNHG1 and SNHG1-regulated genes was constructed. Correlation analysis showed that the risk score based on the expression of the seven genes was significantly correlated with stage, grade, and local tumor stage. Furthermore, the KM survival curve demonstrated that patients in the high-risk group had significantly poorer outcomes compared with those in the low-risk group. A nomogram based on risk score was then constructed to evaluate the probability of 1-year, 3-year, and 5-year overall survival in HCC patients.

In conclusion, taken together, aberrant expression of the cell cycle-related genes is the most significant change in the gene expression patterns in HCC. SNHG1 plays a crucial role in the pathogenesis of HCC by regulating cell cycle-related genes as a ceRNA. A seven-gene signature constructed by SNHG1 and SNHG1-regulated genes is a potential independent prognostic factor for OS of HCC patients.

Acknowledgments

The results published here are in whole based upon data generated by the TCGA Research Network: https://www.cancer.gov/tcga. This work was supported by the National Natural Science Foundation of China (grant no. 82070155).

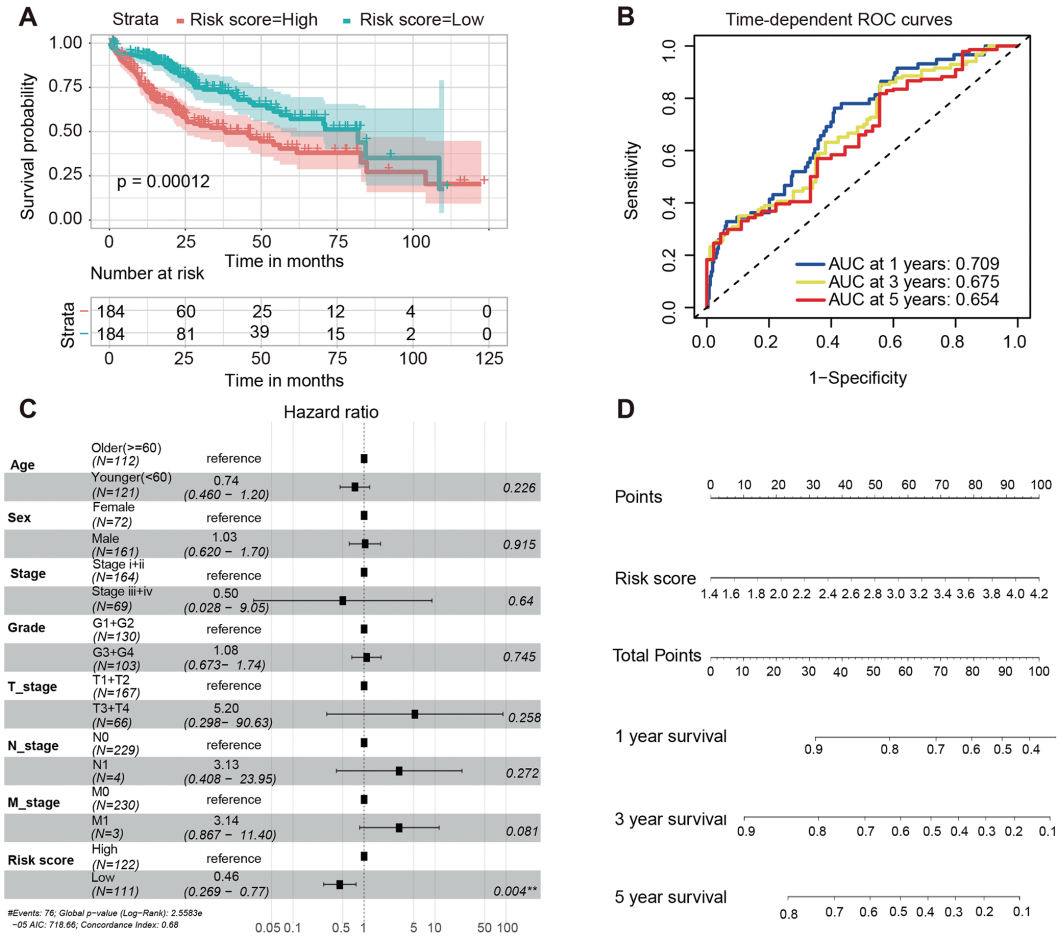

Fig. 8. Construction of a prognostic signature and nomogram prediction model based on the seven genes.
(A) Kaplan-Meier survival curve for the low- and high-risk groups in the TCGA-LIHC dataset. (B) Time-dependent ROC curve analyses of prediction models for 1-, 3- and 5-year survival. (C) Multivariate analyses of the factors associated with OS. (D) A nomogram for predicting the 1-, 3-, and 5-year survival rates.

Conflict of Interest

The authors declare no conflict of interest.

References

Ba, Z., Gu, L., Hao, S., Wang, X., Cheng, Z. & Nie, G. (2018) Downregulation of lncRNA CASC2 facilitates osteosarcoma growth and invasion through miR-181a. *Cell Prolif.*, **51**, e12409.

Bolanos-Garcia, V.M. & Blundell, T.L. (2011) BUB1 and BUBR1: multifaceted kinases of the cell cycle. *Trends Biochem. Sci.*, **36**, 141-150.

Cao, P., Jin, Q., Feng, L., Li, H., Qin, G. & Zhou, G. (2021) Emerging roles and potential clinical applications of noncoding RNAs in hepatocellular carcinoma. *Semin. Cancer Biol.*, **75**, 136-152.

Di Palo, A., Siniscalchi, C., Mosca, N., Russo, A. & Potenza, N. (2020) A novel ceRNA regulatory network involving the long non-coding antisense RNA SPACA6P-AS, miR-125a and its mRNA targets in hepatocarcinoma cells. *Int. J. Mol. Sci.*, **21**, 5068.

Elowe, S. & Bolanos-Garcia, V.M. (2022) The spindle checkpoint proteins BUB1 and BUBR1: (SLiM)ming down to the basics. *Trends Biochem. Sci.*, **47**, 352-366.

Gong, C., Ai, J., Fan, Y., Gao, J., Liu, W., Feng, Q., Liao, W. & Wu, L. (2019) NCAPG promotes the proliferation of hepatocellular carcinoma through PI3K/AKT signaling. *Onco Targets Ther.*, **12**, 8537-8552.

Hara, K., Kinoshita, K., Migita, T., Murakami, K., Shimizu, K., Takeuchi, K., Hirano, T. & Hashimoto, H. (2019) Structural basis of HEAT-kleisin interactions in the human condensin I subcomplex. *EMBO Rep.*, **20**, e47183.

Hayward, D., Alfonso-Perez, T., Cundell, M.J., Hopkins, M., Holder, J., Bancroft, J., Hutter, L.H., Novak, B., Barr, F.A. & Gruneberg, U. (2019) CDK1-CCNB1 creates a spindle checkpoint-permissive state by enabling MPS1 kinetochore localization. *J. Cell Biol.*, **218**, 1182-1199.

Hu, Z.D., Jiang, Y., Sun, H.M., Wang, J.W., Zhai, L.L., Yin, Z.Q. & Yan, J. (2021) KIF11 promotes proliferation of hepatocellular carcinoma among patients with liver cancers. *Biomed Res. Int.*, **2021**, 2676745.

Jin, J., Xu, H., Li, W., Xu, X., Liu, H. & Wei, F. (2020) LINC00346 acts as a competing endogenous RNA regulating development of hepatocellular carcinoma via modulating CDK1/CCNB1 axis. *Front. Bioeng. Biotechnol.*, **8**, 54.

Jin, M., Li, J., Hu, R., Xu, B., Huang, G., Huang, W., Chen, B., He, J. & Cao, Y. (2021) Cyclin A2/cyclin-dependent kinase 1-dependent phosphorylation of Top2a is required for S phase entry during retinal development in zebrafish. *J. Genet.*

Genomics, **48**, 63-74.
Kapanidou, M., Curtis, N.L. & Bolanos-Garcia, V.M. (2017) Cdc20: at the crossroads between chromosome segregation and mitotic exit. *Trends Biochem. Sci.*, **42**, 193-205.
Kong, J., Yu, G., Si, W., Li, G., Chai, J., Liu, Y. & Liu, J. (2022) Identification of a glycolysis-related gene signature for predicting prognosis in patients with hepatocellular carcinoma. *BMC Cancer*, **22**, 142.
Li, B., Li, A., You, Z., Xu, J. & Zhu, S. (2020) Epigenetic silencing of CDKN1A and CDKN2B by SNHG1 promotes the cell cycle, migration and epithelial-mesenchymal transition progression of hepatocellular carcinoma. *Cell Death Dis.*, **11**, 823.
Li, C., Li, R. & Zhang, W. (2018) Progress in non-invasive detection of liver fibrosis. *Cancer Biol. Med.*, **15**, 124-136.
Li, R., Jiang, X., Zhang, Y., Wang, S., Chen, X., Yu, X., Ma, J. & Huang, X. (2019) Cyclin B2 overexpression in human hepatocellular carcinoma is associated with poor prognosis. *Arch. Med. Res.*, **50**, 10-17.
Liu, T., Shi, Q., Yang, L., Wang, S., Song, H., Wang, Z., Xu, X., Liu, H., Zheng, H. & Shen, Z. (2021) Long non-coding RNAs HERH-1 and HERH-4 facilitate cyclin A2 expression and accelerate cell cycle progression in advanced hepatocellular carcinoma. *BMC Cancer*, **21**, 957.
Llovet, J.M., Kelley, R.K., Villanueva, A., Singal, A.G., Pikarsky, E., Roayaie, S., Lencioni, R., Koike, K., Zucman-Rossi, J. & Finn, R.S. (2021) Hepatocellular carcinoma. *Nat. Rev. Dis. Primers*, **7**, 6.
Meng, F., Liu, J., Lu, T., Zang, L., Wang, J., He, Q. & Zhou, A. (2021) SNHG1 knockdown upregulates miR-376a and downregulates FOXK1/Snail axis to prevent tumor growth and metastasis in HCC. *Mol. Ther. Oncolytics*, **21**, 264-277.
Mu, W., Guo, L., Liu, Y., Yang, H., Ning, S. & Lv, G. (2021) Long noncoding RNA SNHG1 regulates LMNB2 expression by sponging miR-326 and promotes cancer growth in hepatocellular carcinoma. *Front. Oncol.*, **11**, 784067.
Nielsen, C.F., Zhang, T., Barisic, M., Kalitsis, P. & Hudson, D.F. (2020) Topoisomerase IIalpha is essential for maintenance of mitotic chromosome structure. *Proc. Natl. Acad. Sci. U. S. A.*, **117**, 12131-12142.
Novak, M., Polak, B., Simunic, J., Boban, Z., Kuzmic, B., Thomae, A.W., Tolic, I.M. & Pavin, N. (2018) The mitotic spindle is chiral due to torques within microtubule bundles. *Nat. Commun.*, **9**, 3571.
Pinero, F., Dirchwolf, M. & Pessoa, M.G. (2020) Biomarkers in hepatocellular carcinoma: diagnosis, prognosis and treatment response assessment. *Cells*, **9**, 1370.
Qiu, J., Zhang, S., Wang, P., Wang, H., Sha, B., Peng, H., Ju, Z., Rao, J. & Lu, L. (2020) BUB1B promotes hepatocellular carcinoma progression via activation of the mTORC1 signaling pathway. *Cancer Med.*, **9**, 8159-8172.
Qu, A. & Yang, Q. (2020) LncRNA SNHG1 promotes cell progression and metastasis via sponging miR-377-3p in hepatocellular carcinoma. *Neoplasma*, **67**, 557-566.
Quinn, J.J. & Chang, H.Y. (2016) Unique features of long non-coding RNA biogenesis and function. *Nat. Rev. Genet.*, **17**, 47-62.
Salmena, L., Poliseno, L., Tay, Y., Kats, L. & Pandolfi, P.P. (2011) A ceRNA hypothesis: the Rosetta Stone of a hidden RNA language? *Cell*, **146**, 353-358.
Sana, J., Faltejskova, P., Svoboda, M. & Slaby, O. (2012) Novel classes of non-coding RNAs and cancer. *J. Transl. Med.*, **10**, 103.
Serpico, A.F., Febbraro, F., Pisauro, C. & Grieco, D. (2022) Compartmentalized control of Cdk1 drives mitotic spindle assembly. *Cell Rep.*, **38**, 110305.
Sun, Y., Wei, G., Luo, H., Wu, W., Skogerbo, G., Luo, J. & Chen, R. (2017) The long noncoding RNA SNHG1 promotes tumor growth through regulating transcription of both local and distal genes. *Oncogene*, **36**, 6774-6783.
Sung, H., Ferlay, J., Siegel, R.L., Laversanne, M., Soerjomataram, I., Jemal, A. & Bray, F. (2021) Global Cancer Statistics 2020: GLOBOCAN estimates of incidence and mortality worldwide for 36 cancers in 185 countries. *CA Cancer J. Clin.*, **71**, 209-249.
Takahashi, K., Yan, I., Haga, H. & Patel, T. (2014) Long noncoding RNA in liver diseases. *Hepatology*, **60**, 744-753.
Tan, Y., Zhang, M., Chen, X. & Deng, Y. (2022) Identifying a three-gene signature and associated drugs for hepatitis B virus-related hepatocellular carcinoma using comprehensive bioinformatics analysis. *Tohoku J. Exp. Med.*, **258**, 149-157.
Thin, K.Z., Tu, J.C. & Raveendran, S. (2019) Long non-coding SNHG1 in cancer. *Clin. Chim. Acta*, **494**, 38-47.
Wang, J. & Zhang, C. (2021) Identification and validation of potential mRNA- microRNA- long-noncoding RNA (mRNA-miRNA-lncRNA) prognostic signature for cervical cancer. *Bioengineered*, **12**, 898-913.
Wong, N., Yeo, W., Wong, W.L., Wong, N.L., Chan, K.Y., Mo, F. K., Koh, J., Chan, S.L., Chan, A.T., Lai, P.B., Ching, A.K., Tong, J.H., Ng, H.K., Johnson, P.J. & To, K.F. (2009) TOP2A overexpression in hepatocellular carcinoma correlates with early age onset, shorter patients survival and chemoresistance. *Int. J. Cancer*, **124**, 644-652.
Xu, B., Xu, T., Liu, H., Min, Q., Wang, S. & Song, Q. (2017) MiR-490-5p suppresses cell proliferation and invasion by targeting BUB1 in hepatocellular carcinoma cells. *Pharmacology*, **100**, 269-282.
Xu, G., Xu, W.Y., Xiao, Y., Jin, B., Du, S.D., Mao, Y.L. & Zhang, Z.T. (2020) The emerging roles of non-coding competing endogenous RNA in hepatocellular carcinoma. *Cancer Cell Int.*, **20**, 496.
Yamamura, S., Imai-Sumida, M., Tanaka, Y. & Dahiya, R. (2018) Interaction and cross-talk between non-coding RNAs. *Cell. Mol. Life Sci.*, **75**, 467-484.
Yang, J., Pan, G., Guan, L., Liu, Z., Wu, Y., Liu, Z., Lu, W., Li, S., Xu, H. & Ouyang, G. (2022) The burden of primary liver cancer caused by specific etiologies from 1990 to 2019 at the global, regional, and national levels. *Cancer Med.*, **11**, 1357-1370.
Yang, L., Yin, W., Liu, X., Li, F., Ma, L., Wang, D. & Li, H. (2021) Identification of a five-gene signature in association with overall survival for hepatocellular carcinoma. *PeerJ*, **9**, e11273.
Zhao, S., Zhang, Y., Lu, X., Ding, H., Han, B., Song, X., Miao, H., Cui, X., Wei, S., Liu, W., Chen, S. & Wang, J. (2021) CDC20 regulates the cell proliferation and radiosensitivity of P53 mutant HCC cells through the Bcl-2/Bax pathway. *Int. J. Biol. Sci.*, **17**, 3608-3621.
Zheng, R., Qu, C., Zhang, S., Zeng, H., Sun, K., Gu, X., Xia, C., Yang, Z., Li, H., Wei, W., Chen, W. & He, J. (2018) Liver cancer incidence and mortality in China: temporal trends and projections to 2030. *Chin. J. Cancer Res.*, **30**, 571-579.

Supplementary Files

Please find supplementary file(s);
https://doi.org/10.1620/tjem.2022.J083